International Journal of Earth, Energy and Environmental Sciences
ISSN: 2517-942X
Vol:7, No:4, 2013

An Evaluation of Digital Elevation Models to Short-Term Monitoring of a High Energy Barrier Island, Northeast Brazil

Venerando E. Amaro, Francisco Gabriel F. de Lima, and Marcelo S.T. Santos

***Abstract*—**The morphological short-term evolution of Ponta do Tubarão Island (PTI) was investigated through high accurate surveys based on post-processed kinematic (PPK) relative positioning on Global Navigation Satellite Systems (GNSS). PTI is part of a barrier island system on a high energy northeast Brazilian coastal environment and also ans area of high environmental sensitivity. Surveys were carried out quarterly over a two years period from May 2010 to May 2012. This paper assesses statically the performance of digital elevation models (DEM) derived from different interpolation methods to represent morphologic features and to quantify volumetric changes and TIN models shown the best results to that purposes. The MDE allowed quantifying surfaces and volumes in detail as well as identifying the most vulnerable segments of the PTI to erosion and/or accumulation of sediments and relate the alterations to climate conditions. The coastal setting and geometry of PTI protects a significant mangrove ecosystem and some oil and gas facilities installed in the vicinities from damaging effects of strong ocean-waves and currents. Thus, the maintenance of PTI is extremely required but the prediction of its longevity is uncertain because results indicate an irregularity of sedimentary balance and a substantial decline in sediment supply to this coastal area.

***Keywords*—**DEM, GNSS, short-term monitoring, Brazil.

I. Introduction

THE Northern Coast of Rio Grande do Norte State (RN) in the northeastern Brazilian coast is characterized by vigorous action of several coastal processes that cause widespread coastal erosion with high range of shoreline retreat and relevant morphologic changes with volumetric variations of sedimentary balance in coastal zone. Recent descriptions highlight notable openings and closures of tidal inlets and tidal channels, barrier islands formation and active dune field motion occurring even in seasonal scale remark. All these morphologic features changes are governed by the dynamic action of the continuous trade winds that promote waves and coastal sediment transport related to eastward drift currents. In turn, these processes are also controlled by semidiurnal mesotidal regime, semi-arid weather conditions and local neotectonic setting. Such coastal processes, coupled with anthropogenic interference (e.g. oil industry, salt ponds, shrimp farms and aeolic parks), cause significant changes to coastal morphology as noticed in multitemporal monitoring studies since interdecadal to relatively short term time interval [1]-[2]-[3]. In this context, the intense action of these coastal dynamic agents caused severe socioeconomic difficulties to the installations of hydrocarbon Exploration Company and represents a serious risk to these coastal ecosystems with high environmental sensitivity index, consisting of estuaries with mangroves, sandy beaches and active dune fields occupied by coastal communities [2].

In order to prevent accidental oil spills and the destruction of the base of oil exploration fields and pipelines it is continuously used rock armor and retaining walls along shoreline against sea erosion and energy of wave impact. Since the beginning of coastal monitoring studies a decade ago it was clear the increase of the size and mass of the riprap material used to contain the destruction, once the facilities are currently in the intertidal zone due to beach erosion and shoreline retreat in a landward direction. This engineering decision based on armoring of shoreline has intensified and accelerated the erosive process of the beach face. Thus, the barriers islands systems, fitted parallel to the coast, are fundamental in preserving industries installed in beach area and also coastal communities nearby estuaries.

The methodological strategy based on multitemporal comparison of geodetic Digital Elevation Models (DEM) has made possible to represent and quantify variations of shoreline and beach face morphology. It as contributes to identify most sensitive erosion areas and erosion/accretion motion patterns that can subsidize adjustment of prognostic models for shoreline changes, assisting in studies on the effects of relative sea level rise, global climatic phenomena, such as El Niño Southern Oscillation, and anthropogenic activities in the changes detected in areas of intense coastal dynamic [4].

In accurate DEM generation, planialtimetric points were collected by Global Navigation Satellite Systems (GNSS) and subjected to interpolation process in which points are estimated from ground sampling points. Such sampling of points must be compatible, in number and spatial distribution, with beach morphology. The more morphological features are found on beach face, more sampling points must be collected, always trying to avoid the subsampling and redundant sampling points.

Venerando E. Amaro is with the Department of Geology, Federal University of Rio Grande do Norte, Natal, RN, CEP 59072-970, Brazil (phone: 55.84.3215.3212; e-mail: amaro@geologia.ufrn.br).

Francisco. G. F. Lima is with the Department of Geology, Federal University of Rio Grande do Norte, Natal, RN, CEP 59072-970, Brazil (e-mail:gabrielfleng@gmail.com).

Marcelo S. T. Santos is with Department of Geology, Federal University of Recôncavo da Bahia, Cruz das Almas, BA, Brazil (e-mail: mstsantos@yahoo.com.br).

II. Study Area

A. Location

The study area comprises the Ponta do Tubarão Island (hereinafter referred to PTI) and surroundings that is part of a barrier islands system that is inserted in Ponta do Tubarão Sustainable Development Reserve, whose environmental configuration includes oceanic sandy beaches, tidal channels, tidal inlets, sandy-muddy plains with mangrove swamps and active dune fields (Fig. 1). The PTI is located frontally and parallel to the eastern half of Soledade Beach where are installed oil-producing wells, pipelines, oil and natural gas storage stations and wind towers. This geometric configuration helps to protect Soledade Beach, estuarine mangrove ecosystems and villages of Barreiras and Diogo Lopes from the dynamic action of ocean waves and currents.

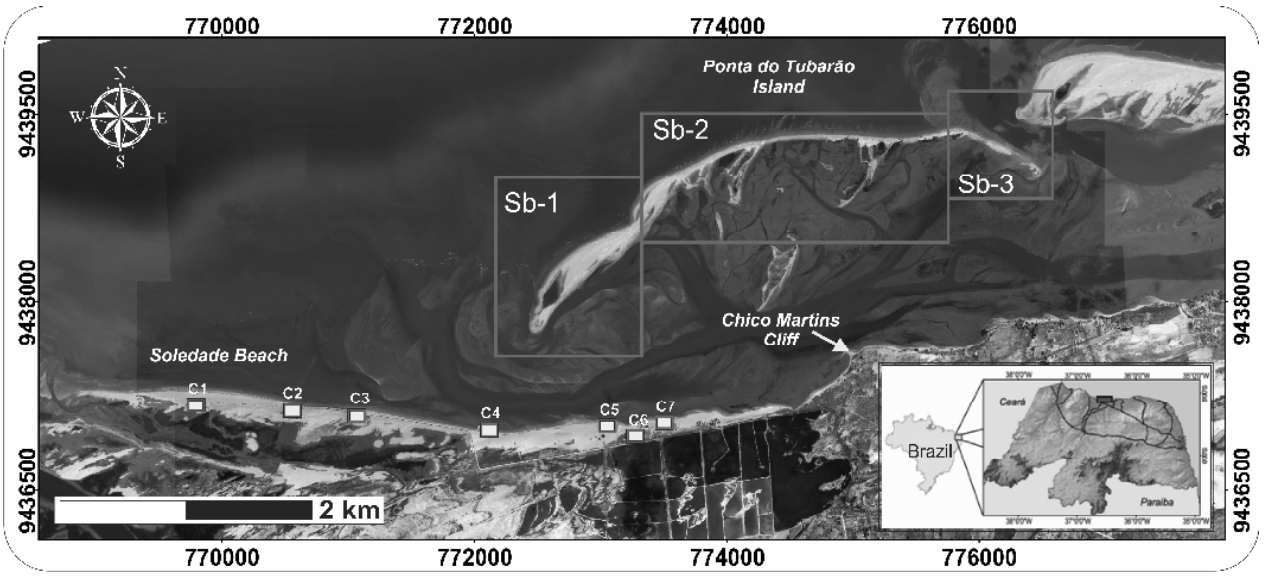

Fig. 1 Location of the study area, main access roads and localities
Ponta do Tubarão Island was subdivided into three subareas: Sb-1, Sb-2 e Sb-3. Onshore oil and gas production facilities in Soledade Beach: C1 – Base Serra A; C2 – Base Serra B; C3 – Base Serra C; C4 – Base Serra E; C5 – Base Macau 14; C6 – Oil and Gas Collection Station of Macau A; C7 – Base Macau 15.

B. Geological Setting

The EW-trend orientation and shape of shorelines are resulting from the combined action of the structural control of Carnaubais-Afonso Bezerra fault system, longshore drift from W to E that carries sediment parallel to the shore, and trade winds mainly from SE to NE, which promote intense morphological modification of area-to-volume ratio of sediment [5]. Geologically, the study area is part of Potiguar Basin that was formed after the breakup of the continental crust of the Gondwana supercontinent, which resulted in Neocomian NE-trend architecture of the rift. The Precambrian shear zones of NE-trend were reactivated from the Cretaceous to the Cenozoic and controlled successive episodes of deposition [6], where Cretaceous sedimentary strata were deposited and covered by deposits of Tertiary and Quaternary age. Holocene deposits on the coast are composed predominantly by sediments from depositional processes active in the present day such as alluvial fans, beach-dunes system sediments, tidal flat and sandy-muddy drape. In general terms, the IPT is composed mainly of wind-sand deposits and mangroves that develop mainly over the more stable parts of the island on the sandy-muddy flat deposits facing the estuary [7].

C. Climate Scenario

The Northeast Brazil is characterized by high incidence of solar radiation, with uniform thermal regime marked by maximum temperatures above 40°C and average temperatures of 25° C throughout the year. The daily temperature range is usually between 8° to 10°C. The climate of the region is hot semi-arid type *BSh* using the Köppen-Geiger system. Annual rainfall is less than 750 mm with periods of drought which last from 7 to 8 months, normally from June to January. The influence of thermal anomalies of Pacific waters, and possibly teleconnection pattern due to the Walker cell with the Tropical South Atlantic, in the control of the precipitation in northeastern Brazil has been described by many authors, e.g. [8]. The general comparison between the climate normal from 1961 to 1990, provided by the Macau Meteorological Station-A317 of the National Institute of Meteorology of Brazil (INMET) showed that strong drought events seems to be connected with the El Niño Southern Oscillation phenomena, such as in the years 2010 to 2012, and in the same way, the wettest years present good correlation with the La Niña anomaly.

The main atmospheric system active in the study area is the Intertropical Convergence Zone formed by the junction of the

trade winds from NE and SE. The average wind speed was 4,81 ± 2,0 m/s from January 2010 to May 2012 was with directions ranging from NE, E, and SE. NE trade winds are stronger and lead the longshore drift. The highest average wind speed occurred between August and November, with a peak in September (6.5 ± 2.0 m/s), with predominance of easterly (August and September) and northeasterly (October and November) trade winds. These seasonal oscillations of trade winds control the preferred *direction* of propagation of the *incident wave*, largely from NE.

It was observed significant wave height average ranging from 0.74 to 1.15 m and period average around 11s from December 2010 to February 2011 [9]. Wave periods with lower values were observed mainly between May and August. The coastal circulation is dominated by tidal currents and longshore drift, with a maximum speed of 97 cm/s mostly westward during rising tide and towards the north (oblique to the coast) with a maximum of 50 cm/s during falling tide. Thus, strong oblique trade winds and longshore currents that generate oblique breaking waves result in sediment transport at about $100m^3$/day and extensive spits formation parallel to the EW-trend coast [10]. Tides have a mesotidal semi-diurnal regime.

III. Material and Methods

Currently geodetic analysis of erosion/accretion on shorelines involves high accuracies. For these purposes the methodology was based on monitoring the state of the coastal system on PTI by means of geodetic surveys in seasonal short-term approach using a post-processed kinematic (PPK) relative positioning GPS technique of high accuracy established by [3]-[4]-[11]-[12]. This procedure enabled analysis of sedimentary variations in both seasonal (from May 2011 to May 2012) and interannual (between May 2010 and May 2012) short-term range. Data from monitoring surveys provided the input for the geostatistical interpolator evaluation and numerical models classification for accurate comparison of beach morphology behavior. The fieldwork was conducted in five campaigns from May 2011 to May 2012, always during neap tide. As the detection of shoreline changes depends on a steady measurement technique position of a particular tidal-based vertical reference datum, the dry-wet interface selected was that when the water level at that point was at a mean high water. A GPS system was mounted on a quad bike and the profiles then were carried out following these dry-wet lines around the island, and along and crossing the main morphological features. The receivers used were of the Trimble R3 model that tracks carrier phase observations in L1 frequency having nominal horizontal accuracy of 5 mm + 1 ppm and vertical of 5 mm + 2 ppm. The PPK stations were distributed along the survey island, in order to not to exceed the maximum 3.5 km range from the nearest base station [3]. The meteorological data of winds, rainfall and temperature were obtained from the Macau Meteorological Station-A317 (located at 5.1150°S and 36.7156°W 4 m above sea level).

The study area corresponds to 540,136 m² and was raised with 7,115 sampling points in 2h10min, resulting in a density of 54.73 points/min or 132.48 points/hectare. The acceptable standard error was 10 cm for vectors and with 68% confidence level. Thus, the geodetic coordinates for each sample point with their respective standard errors were obtained as results. The orthometric height was calculated from geometric height as established by [3]-[13]-[14]. In order to check the interpolation method which results in DEM most appropriate to represent beach morphology in highly dynamic coastal environment, during the surveys 28 ground control points were also collected in fast static mode. In this way, altitudes on each ground control point were compared with their homologous on the DEM generated. Based on statistical analysis of discrepancies between both heights values, were undertaken accuracy, precision and trend analysis. In this work the adopted standard followed the technical rules, specifications and procedures of the Regulatory National Cartography (Brazil, 1984) which define the Cartographic Accuracy Standard (PEC in Portuguese) as the Law Decree no. 89,817/1984. PEC is a statistical indicator of dispersion quality of geometric accuracy on cartographic documents applied both for planimetric as altimetric valuations. According to PEC, 90% of the isolated points obtained by interpolation must achieve a standard value as well as a limit value for the Mean Square Error when compared to the ground check points.

IV. Results and Discussion

A. Evaluation and Classification of DEM

In survey with GNSS positioning by means of PPK mode it was admitted only solutions with fixing the integer ambiguities of less than 5 cm in vectors with up to 3.5 km. In the generation of DEM to PTI were evaluated those obtained by seven interpolation methods: Inverse Distance Weighted (IDW), Kriging, Spline, Triangulated Irregular Network (TIN), Top to Raster (TtR), Trend and Natural Neighbor (NN). In assessing the DEM accuracy identify what methods were the most adjusted to this coastal segment design representation. The statistical discrepancy was used to evaluate the reliability of heights measured in models and those on homologous ground control points (Table I). The methods Spline, TIN, TtR and NN had decimetric accuracy satisfactory to coastal monitoring and other numerous applications. However, only methods TtR, NN and TIN offered DEM consistent with ground truth, highlighting delineations of the smooth transitions of valleys between dunes, berms and beach cusps of metric size. The first two are quite similar to DEM generated by TIN method but both tended to smoothing of surfaces.

TABLE I
STATISTICAL DATA OF DIGITAL ELEVATION MODELS OBTAINED BY DIFFERENT INTERPOLATION METHODS
STATISTICAL DISCREPANCY OF HIGHTS OBTAINED FROM MODELS RELATED TO GROUND CONTROL POINTS (GCP)

Interpolation Methods	Mean	Standard Deviation	Median	RMSE	Coefficient R^2	Visual Coherence	Statistical Discrepancy Related to GCP		
							Mean	SD	RMS
GCP	2.283	0.460	2.276	-	-	-	-	-	-
IDW	2.19	0.373	2.213	0.234	0.778	Good	0.093	0.219	0.234
Krigagem	2.151	0.362	2.174	0.323	0.57459	Good	0.132	0.301	0.323
Spline	2.300	0.450	2.269	0.102	0.952	Bad	-0.010	0.103	0.102
TIN	2.266	0.410	2.246	0.104	0.954	Good	0.016	0.105	0.104
TtR	2.265	0.413	2.312	0.139	0.91	Good	0.017	0.140	0.139
Trend	1.926	0.167	1.962	0.577	0.03	Bad	0.357	0.461	0.577
NN	2.224	0.389	2.194	0.104	0.954	Good	0.059	0.136	0.146

RMSE: Root Mean Square Error. IDW: Inverse Distance Weighted. TIN: Triangulated Irregular Network. TtR: Top to Raster. NN: Natural Neighbor.

TIN model achieved a more realistic terrain representation without any surface attenuation, clearly better representing geomorphologic features of PTI (Fig. 2). Likewise, TIN model attained better accuracy performance when compared to those generated by TtR and VN, with less difference between measured and interpolated heights for 58% of homologous ground control points. TIN model had a smaller mean error (0.080) and accumulated error (2.247), featuring the best correlation of the three methods (R^2_{TIN} = 95,4%; R^2_{Topo} = 91%; R^2_{VizNat} = 92,7%), mean, median and standard deviation very close to the values of ground points.

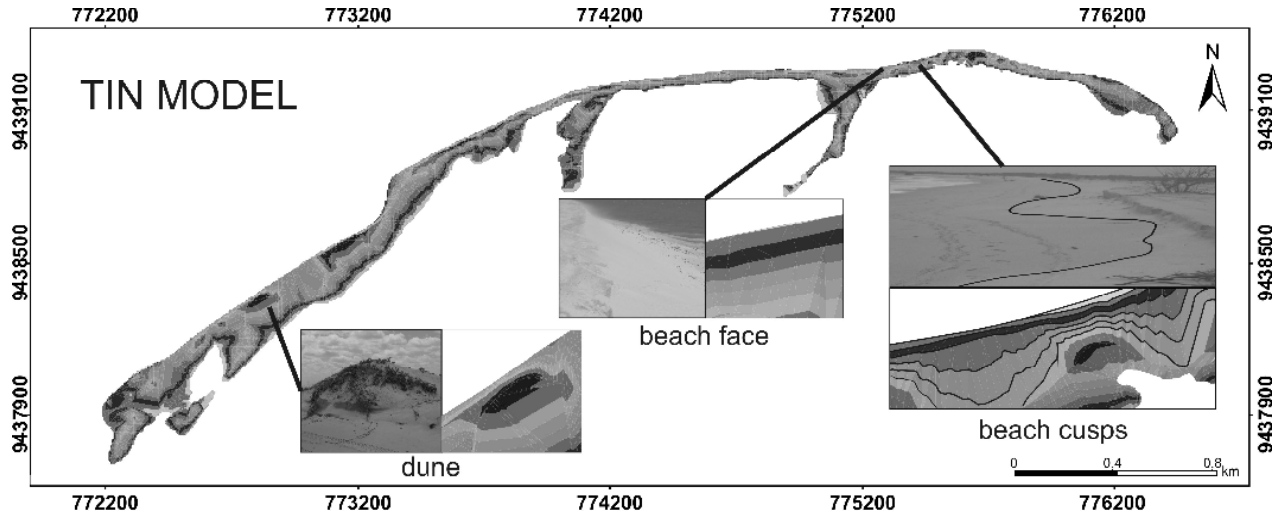

Fig. 2 Digital elevation model obtained by TIN interpolator for Ponta do Tubarão Island. DEM presents curves consistent with meso and macro scale morphologies such as beach face, dunes and beach cusps

Analysis of accuracy, precision and trend were made to DEM generated by methods TIN, TtR and NN on the scale of 1:1,000 and with contour lines equal to 0.50 m, corresponding to Class A of PEC (Table II). Analysis of accuracy showed Student's t values (t_{TIN} = -11.792; t_{TtR} = -8.807; t_{NN} = -7.451) smaller than the tabulated Student's t values [$t_{(27;\ 0,10)TIN} = t_{(27;\ 0,10)TtR} = t_{(27;\ 0,10)NN}$ = -1.314]. Thus, population averages of errors in altimetric data calculated by (1) ($\mu_{TIN} < 4.2$ cm; $\mu_{TtR} < 5.2$ cm; $\mu_{VN} = 9.2$ cm) were statistically less than or equal to the acceptable error in accuracy (25 cm for Class A).

$$\mu \leq \bar{x} + (t_{\alpha})\left(\frac{s}{\sqrt{n}}\right) \quad (1)$$

where, $\bar{x}$: sample average; *s*: sample standard deviation; α: significance level; t_{α}: *value distribution of Student;* n: sample size.

The Chi-squared values to TIN and NN (χ^2_{TIN}=10.716; χ^2_{VN} = 17.978) were lower than tabulated Chi-squared values ($\chi^2_{(27;0,10)TIN} = \chi^2_{(27;0,10)VN}$ = 18.114). Hence, the population deviations calculated in (2) were statistically less than or equal to the acceptable error in precision (16.7 cm for Class A).

$$\sigma \leq \sqrt{\frac{(n-1).s^2}{\chi^2_{1-\alpha}}} \quad (2)$$

where, s: sample standard deviation; 1−α: confidence interval; $\chi^2_{1-\alpha}$: Chi-square distribution value; *n* : sample size.

In trend analysis, Student's t values based on (3) and related to models TIN [$t_{(27;\ 0,05)}$ = 0.823] and TtR [$t_{(27;\ 0,05)}$ = 0.646], are between the limits of tabulated Student's t (-1.703 ≤ t ≤ 1.703) indicating that models are no trend.

$$t_{\alpha/2} = \frac{\bar{x}}{s}\sqrt{n} \quad (3)$$

where, $t_{\alpha/2}$: point $100_{\alpha/2}$% superior of the student's t-distribution; n : sample size.

TABLE II
ANALYSIS OF ACCURACY, PRECISION AND TREND TO TIN, TTR AND NN INTERPOLATION METHODS ON THE SCALE OF 1:1,000 AND CORRESPONDING TO CLASS A OF CARTOGRAPHIC ACCURACY STANDARD (PEC)

	Interpolation Methods		
	TIN	TtR	NN
$\bar{x}$: Mean	0.016	0.017	0.059
s : Standard Deviation	0.105	0.140	0.136
n (sample number)	28	28	28
SE: Class A	0.167	0.167	0.167
PEC: Class A	0.250	0.250	0.250
μ	0.042	0.052	0.092
Σ	0.128	0.171	0.166
Analysis of Accuracy			
$t_{(27;\ 0,10)}$ (t tab)	1.314	1.314	1.314
$t_{calculated}$ (t calc)	-11.,792	-8.807	-7.451
Conclusion	tcalc<ttab Acceptable	tcalc<ttab Acceptable	tcalc<ttab Acceptable
Analysis of Precision			
$\chi^2_{(27;\ 0,10)}$ (χ^2 tab)	18.114	18.114	18.114
$\chi^2_{(calculated)}$ (χ^2 tab)	10.716	19.051	17.978
Conclusion	χ^2calc<χ^2tab Acceptable	χ^2calc>χ^2tab Unacceptable	χ^2calc<χ^2tab Acceptable
Trend Analysis			
$t_{(27;\ 0,05)}$ (t tab)	1.703	1.703	1.703
$t_{(calculated)}$ (t calc)	0.806	0.643	2.276
Conclusion	tcalc<ttab Acceptable	tcalc<ttab Acceptable	tcalc>ttab Unacceptable

SE: Standard Error. IDW: Inverse Distance Weighted. TIN: Triangulated Irregular Network. TtR: Top to Raster. NN: Natural Neighbor.

Consequently, according to PEC only DEM from TIN interpolation method can be classified as Class A in terms of precision and accuracy and was free from tendency, for a 90% confidence level. Some authors suggested to perform a precise assessment of altimetric PEC checking if 90% of the samples had residue below the values determined for a given scale [15]-[16]-[17]. For this work concerning Class A it corresponds to half the equidistance between contour lines of 0.5 m, which means specified error of 0.25 m. The models generated by methods TIN and TtR presented just 1 ground control point with discrepancy greater than this value and so in accordance with the specifications for Class A.

B. Volumetric Sedimentary Balance

The results relating to analysis of recent PTI morphology evolution based on quarterly GNSS geodetic surveys in PPK mode between May 2011 and May 2012 (herein named Cycle 2) were compared to the results obtained by [12] for quarterly surveys between May 2010 and May 2011 (Cycle 1). Two episodes were estimated in an annual cycle related to sedimentary dynamics on exposed sandy beaches of PTI [11]-[12], based on [18]: a constructive phase, between March and July, with accumulation of sediment on beach face, increase of beach sediment stock, and beach profiles indicating a morphodynamic reflective stage; and a destructive phase, between August and February, marked by sediment removal from beach face and consequent reduction of beach sediment stock, shoreline retreat and morphodynamic behavior towards dissipative stage. Therefore, the analyses of planialtimetric models for Cycle 2 surveys made it possible to understand the behavior of PTI over four monitoring intervals: interval I1 (May to August 2011), interval I2 (August to November 2011), interval I3 (November 2011 to February 2012), and interval I4 (February to May 2012). The main differences between results for Cycle 1 [11]-[12] and results pointed by Cycle 2 surveys are showed on Table III.

TABLE III
DIFFERENCES BETWEEN SURVEYS OF CYCLE 1 AND SURVEYS CARRIED OUT ON CYCLE 2

	Planimetric Balance (m^2)		Volumetric Balance (m^3)	
	May 2010 to May 2011	May 2011 to May 2012	May 2010 to May 2011	May 2011 to May 2012
I1	80,408	2,828	103,739	54,158
I2	-113,205	14,091	-138,591	25,985
I3	75,613	27,242	49,564	-17,625
I4	4,858	-53,224	54,445	-14,716
Annual balance	47,674	-9,063	69,157	47,802

I: Intervals.

The monitoring interval I1 presented total volume of accretion of 54,171 m^3 owing to sediments transported by hydrodynamics in shoreline and action of winds inside the island. More intense accretion was observed in the far west of segment Sb-1 and portions of exposed beaches on segments Sb-1 and Sb-2. During this period, more intense erosion occurred in some flat portions of Sb-1 near the estuary and in boundary between segments Sb-2 and Sb-3.

For interval I2, total volumetric accretion was of 25,985 m^3, correlate to accretion of 176,357 m^3 and 150,372 m^3 of erosion. This positive result reflects the predominance of hydrodynamic processes on shoreline over the wind transport to inland. The main gains were concentrated near tidal channel and exposed beaches of segment Sb-1 and in estuarine portion of segment Sb-2, while the major losses were on exposed beaches along the remaining exposed island and tidal channel of segment Sb-3.

In the third monitoring interval (I3) even showing

planimetric accretion recorded total volumetric erosion of 17,625 m^3, related to 201,530 m^3 of accretion and 219,155 m^3 of erosion. It means the island became topographically lower, but more elongated. The negative volumetric balance for this period is the result of intense action of NE winds and high dynamic of waves, currents and tides. While strong winds transported sediments towards the ocean and consequently flattened the topography, the waves and longshore drift led to more western portions increasing the area of PTI. Major erosion occurred in exposed beaches of PTI as a whole, as well as in tidal channel of segment Sb-3. Some accretion was noted in estuarine mud flat areas and near tidal channel of Sb-1.

In the period I4 occurred total volumetric erosion of 14,716 m^3 connected to 194,323 m^3 of accretion and 209,039 m^3 of erosion resulting from the combined action of waves, currents and strong NE winds. In this interval, increases of sediments occurred essentially near estuarine and tidal channels portion of PTI, while erosion struck mainly exposed beaches of segments Sb-1 and Sb-2.

Likewise, for both short-term cycles of monitoring the planimetric and volumetric analysis showed total positive sedimentary balance, with additions of 38,614 m^2 and 116,959 m^3 of sediments to PTI, respectively. However this scenario can be quickly reversed, because the results found in quarterly and annual intervals indicate less available sediment to PTI for each cycle.

C. Migration Mechanism

During the whole Cycle 1, marked by severe drought, the winds presented a uniform behavior during all ranges studied, taking place now, now of NE, which made it easy to identify their influence on coastal landscape evolution for each one of directional components. This same constancy of winds was only observed in interval I1 of Cycle 2 but there was a lot of rain that watering the exposed sediments of PTI, impeding their transport by wind.

The sedimentary dynamics due to winds in both meso and macro scale occurred mainly in the interior of the island, since along the shoreline this process is chiefly controlled by the dynamics of waves, currents and tides (Fig. 3e). During episodes of prevalence of NE winds, there were larger accumulations of sediments in PTI mud flat segments. In the intervals with predominance of southeasterly winds sediments were transported to the exposed beaches and then removed by longshore drift to nearby tidal channel of subarea Sb-1. Over two monitored cycles, due to this process the island increase of nearly 1.3 km to SW, 640 m at the extreme point.

Some authors pointed out that between November 2010 and January 2011, the most frequent waves were from NNE and NE with mean period of 8s and significant height of 0.9 m, reaching up to 22.8s and 2.2 m [19]. These were energy and time enough to overwash the PTI (Fig. 3a), mostly concave segment Sb-2 (Fig. 3b), typically during months when some segments are topographically lowered. The beach sediments are transported from exposed areas towards the estuary and adhered to muddy substrate of intertidal deposits where seedlings of mangrove species fixate (Fig. 3d). Thus, the joint performance of meteorological and oceanographic forcing caused the PTI to lose initial concavity and become increasingly parallel to the coastline during the monitored cycles (Fig. 3e).

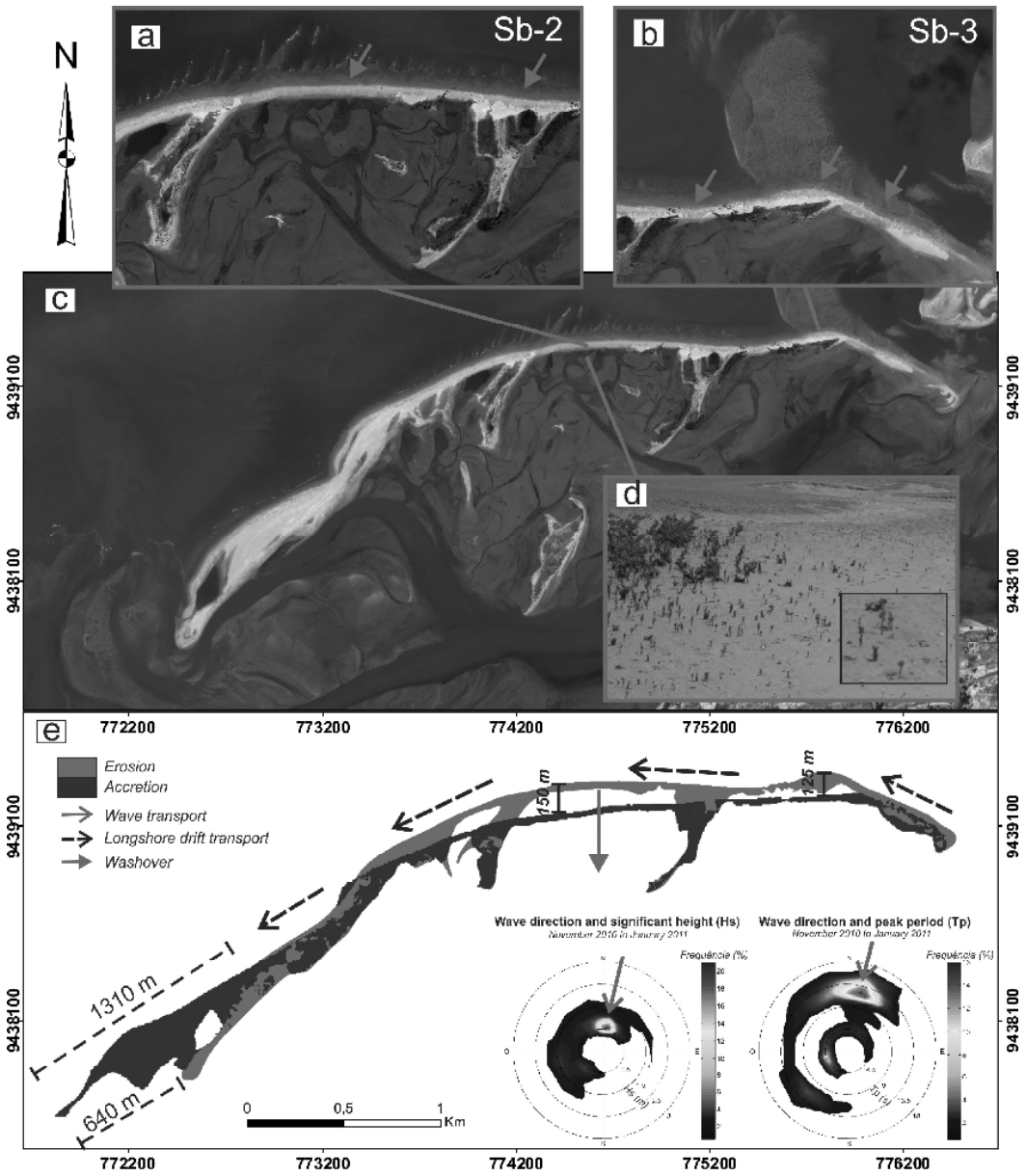

Fig. 3 Migration mechanism of Ponta do Tubarão Island influenced by waves, longshore drift and trade winds
Fig. 3 (a) and (b) show segments often overwashed. Fig. 3 (c) present an overview of the island. Fig.3 (d) emphasizes mud flat areas with seedlings of mangrove. Fig. 3 (e) NE waves transpose the barrier island and force it to move southward; longshore drift carries sediment and favors the migration of the island to SW.

V. Conclusions

In the evaluation of the most appropriate interpolator method to obtain accurate DEM based on GNSS positioning by means of PPK mode to better represent PTI morphology of high sedimentary dynamic, seven interpolation methods were tested: IDW, Kriging, Spline, TIN, Trend, TtR and NN. Such interpolators were evaluated through 28 ground control points randomly selected to check the most suitable to characterize beach morphology and meso and macro features in highly dynamic coastal zone.

The models that presented better accuracy (decimetric gauge) and performed in accordance with ground truth were TIN, TtR and NN models. In order to confirm the results, statistical analyses were made for accuracy, precision and trend, and focused on digital cartographic representation on 1:1,000 scale and with vertical equidistance of 0.5 m related to PEC rules. The model generated by TIN was ranked statistically as Class A in accuracy and precision, also being free from systematic errors. It also showed the best visual performance to represented beach features such dunes and

beach cusps.

The short-term monitoring of planimetric and volumetric morphological changes of PTI were executed quarterly in two episodes called Cycle 1 (May 2010 to May 2011) and Cycle 2 (May 2011 to May 2012), respecting principles of good spatial distribution and high-precision acquisition of geodetic points on PTI in total. The main reason is because generated DEM should represent on relatively flat relief with higher heights concentrated in central portions of PTI. The segments dominated by tidal channels and mud flat areas near estuary are topographically lower.

The volumetric sedimentary balance of Cycle 2 differs from the results of Cycle 1 showing shifts in seasonal settings and 30% drop in annual sediment accretion conditions. This difference was explained by the influence of climate conditions and action of the strong NE winds allied with hydrodynamic regime.

When the main winds are from NE sediments accumulate in areas near the estuary. However, when under the influence of southeasterly winds there is accumulation of sediments in the exposed beaches which are transported by longshore drift to west. For PTI this mechanism was responsible for relevant migration of 0.64 to 1.3 km to southwest in less than 2 years (Fig. 3e). The continuous overwash of some segments of PTI as central segment Sb-2 favor the sediment transport from the beach to the estuary leading to migration of PTI in 150 m southward in 2 years of monitoring.

The expressive growth of IPT for SW has currently favored the maintenance of oil facilities lodged along Soledade Beach, another barrier island/sand spit area, since it has increased protection from destructive effects of intense ocean-waves. However, one should pay attention for the irregularity of sedimentary balance in each short-term cycle. Similarly to the substantial decline in sediment supply to this coastal area already described for seasonal, inter-annual and interdecadal monitoring cycles.

REFERENCES

[1] M.V.S. Souto, A.F. Castro, A.M. Grigio, V.E. Amaro, H. Vital, "Multitemporal Analysis of Geoenvironmental Elements of the Coastal Dynamics of the region of the Ponta do Tubarão, City of Macau/RN, on the basis of remote sensing products and integration in GIS," Journal of Coastal Research, vol.39, p.1618-1621, 2004.

[2] A.M. Grigio, M.V.S. Souto, A.F. Castro, V.E. Amaro, H. Vital, M.A. Iodato, "Method of analysis of the coastline evolution based in remote sensing and geographical information system products: Guamaré District Rio Grande do Norte - Northeast of Brazil," Journal of Coastal Research, vol. 42, no.2, p.412- 421, 2005.

[3] M.S.T. Santos, and V.E. Amaro, "Rede Geodésica para o Levantamento Costeiro do Litoral Setentrional do Rio Grande do Norte," Boletim de Ciências Geodésicas, vol. 17, no. 4, p. 571-585, 2011.

[4] V.E. Amaro, M.S. T. Santos, and M.V.S. Souto, "Geotecnologias Aplicadas ao Monitoramento Costeiro: Sensoriamento Remoto e Geodésia de Precisão," 1st ed., Edition by authors, Natal, 2012.

[5] D.R. Valentim da Silva, V.E. Amaro, M.V.S. Souto, M.C. Nascimento, B.R.B. de Barros Pereira, "Geomorfologia de uma área com alta sensibilidade ambiental na Bacia Potiguar (NE do Brasil)," Universidade Federal do Rio Grande do Norte, Programa de Pós-graduação em Geodinâmica e Geofísica. Revista da Gestão Costeira Integrada, vol. 10, no. 4, p. 545-566, 2010.

[6] N.P Pedrosa Jr., D.L. Castro and J.P.L. Matos, "Assinaturas Magnéticas e Gravimétricas do Arcabouço Estrutural da Bacia Potiguar Emersa, NE do Brasil," Revista Brasileira de Geofísica, vol. 28, no. 2, p. 265-278, 2010.

[7] S.T.P.L. Dantas, and V. E. Amaro, "Caracterização Físico-Química e avaliação das concentrações de elementos maiores e traços em sedimentos arenolamosos do estuário de Diogo Lopes, litoral setentrional do Rio Grande do Norte, Brasil," Revista de Geologia, vol. 25, p. 101-114. 2012.

[8] R. V. Andreoli, and M.T.Kayano, "A importância relativa do Atlântico Tropical Sul e Pacífico Leste na variabilidade de precipitação do Nordeste do Brasil," Revista Brasileira de Meteorologia, vol.22, n.1, 63-74, 2007.

[9] M. F. A. Matos, C. J. E. M. Fortes, V. E. Amaro, A. C. Scudelari, "Avaliação do modelo SWAN na modelação da agitação marítima no litoral setentrional do Rio Grande do Norte-BR," In: 11º Congresso da Água, 2012, Porto. 11º Congresso da Água.

[10] H. Vital, V.E. Amaro, I. M. Silveira, "Coastal erosion on the Rio Grande do Norte State (Northeastern Brazil): Causes and factor versus effects associated processes," Journal of Coastal Research, vol.25, suppl. 1, p. 37-48, SI39:1307-1310, 2006.

[11] M.S.T. Santos, V.E. Amaro, and M.V.S. Souto, "Metodologia geodésica para levantamento de Linha de Costa e Modelagem Digital de Elevação de praias arenosas em estudos de precisão de geomorfologia e dinâmica costeira," Revista Brasileira de Cartografia, vol. 63, p. 663-681, 2011.

[12] M.S.T. Santos, V.E. Amaro, A.T. Silva Ferreira, A.L.S. Santos, "Mapeamento de precisão da dinâmica costeira de curta duração em áreas de alta taxa de erosão no Nordeste do Brasil," Revista de Geologia, vol. 25, p. 7-19, 2012.

[13] W.E. Featherstone, M.C. Dentith, and J.F. Kirby, "Strategies for the accurated determination of orthometric heights from GPS," Survey Review, vol.34, p.278-295, 1998.

[14] M. Ollikainen, "Accuracy of GPS leveling," in 1998 *Proc.* The XIII General Meeting of the Nordic Geodetic Commission. Sweden, vol. 1, p.25-29.

[15] O. R. Vergara, J. P. Cintra, and J. C. L. D'alge, "Avaliação da exatidão cartográfica de documentos atualizados com imagens orbitais e sistemas de informação geográfica," In: XX Congresso Brasileiro de Cartografia, 2001, Porto Alegre

[16] J. M. Souza and R. E. N. Loch, "Refinamento do Modelo Digital de Elevação da Shuttle RADAR Topography Mission - SRTM e sua qualidade cartográfica," In: Congresso Brasileiro de Cadastro Técnico Multifinalitário, Universidade Federal de Santa Catarina, 2008, Florianópolis.

[17] A. P. Santos and C. A. O. Vieira, "Avaliação do Padrão de Exatidão Cartográfica em imagens orbitais IKONOS e CBERS-2B, na Bacia do Ribeirão São Bartolomeu em Viçosa-MG," in 2009 *Proc.* XIV Simpósio Brasileiro de Sensoriamento Remoto, Natal, p. 1021-1030.

[18] L.D. Wright, and A.D. Short, "Morphodynamic variability of surf zones and beaches: a synthesis," Marine Geology, vol. 56, p. 93-118, 1984.

[19] F.G.F. Lima, V.E. Amaro, A.L.S. Santos, M.S.T. Santos. "Avaliação de Métodos de Interpolação na Geração de Modelos Digitais de Elevação de Precisão em Zonas Costeiras de Alta Dinâmica Sedimentar," (Geoscience periodic), submitted for publication.

Dr. Venerando E. Amaro is an Associated Professor since 1990 at the Department of Geology, Federal University of Rio Grande do Norte, Natal, Brazil. Dr. Amaro has spent the last 12 years working in environmental monitoring on coastal zones, mainly south Atlantic environments. He received his M.Sc. degree from University of Brasília, Brazil, and his Doctor in Geosciences degree from the University of São Paulo (Brazil) – Université de Lyon (France). His current research involves applying and developing Geoprocessing techniques in environmental sciences and coastal monitoring.

Francisco G. F. de Lima received his Bachelor's degree in Geology from the Department of Geology, Federal University of Rio Grande do Norte, Natal, Brazil.

Dr. Marcelo S.T. Santos received his M.Sc. degree from University of São Paulo, Brazil, and his Doctor in Petroleum Engineer degree from the Federal University of Rio Grande do Norte, Brazil.